GSA Data Repository Item 2016174
Khajavi, N., Langridge, R.M., Quigley, M.C., Smart, C., Rezanejad, A., and González, F.M., 2016, Late Holocene rupture behaviour and earthquake chronology on the Hope fault, New Zealand: GSA Bulletin, doi:10.1130/B31199.1.

Supplementary Information

This file is composed of 7 main parts: 1) A picture of the extracted seeds from one peat sample; 2) Details of the Matagouri bush on the low gradient Holocene fan; 3) Pit logs and their interpretations; 4) Details of the Schmidt hammering technique; 5) Pictures of the fault bend and the basin formed behind it east of the trench site; 6) Parakeet Stream data; and 7) details of calculating mean recurrence interval (MRI) and its uncertainty.

Part. 1

Supplementary data regarding peat samples

Seeds in a peat sample

We tried to select the most suitable materials for radiocarbon dating including small twigs, leaves, and seeds from every peat sample. If we couldn't find such materials, we selected bigger woody fragments and if none of the above existed, a bulk sample of peat or some rooty fragments were submitted for dating.

Fig. DR1. Beech seeds extracted from peat samples for dating (scale bar in mm). As the seeds were small, five to six seeds were submitted to reach the necessary sample mass.

Part. 2

Supplementary surface data

Matagouri bush

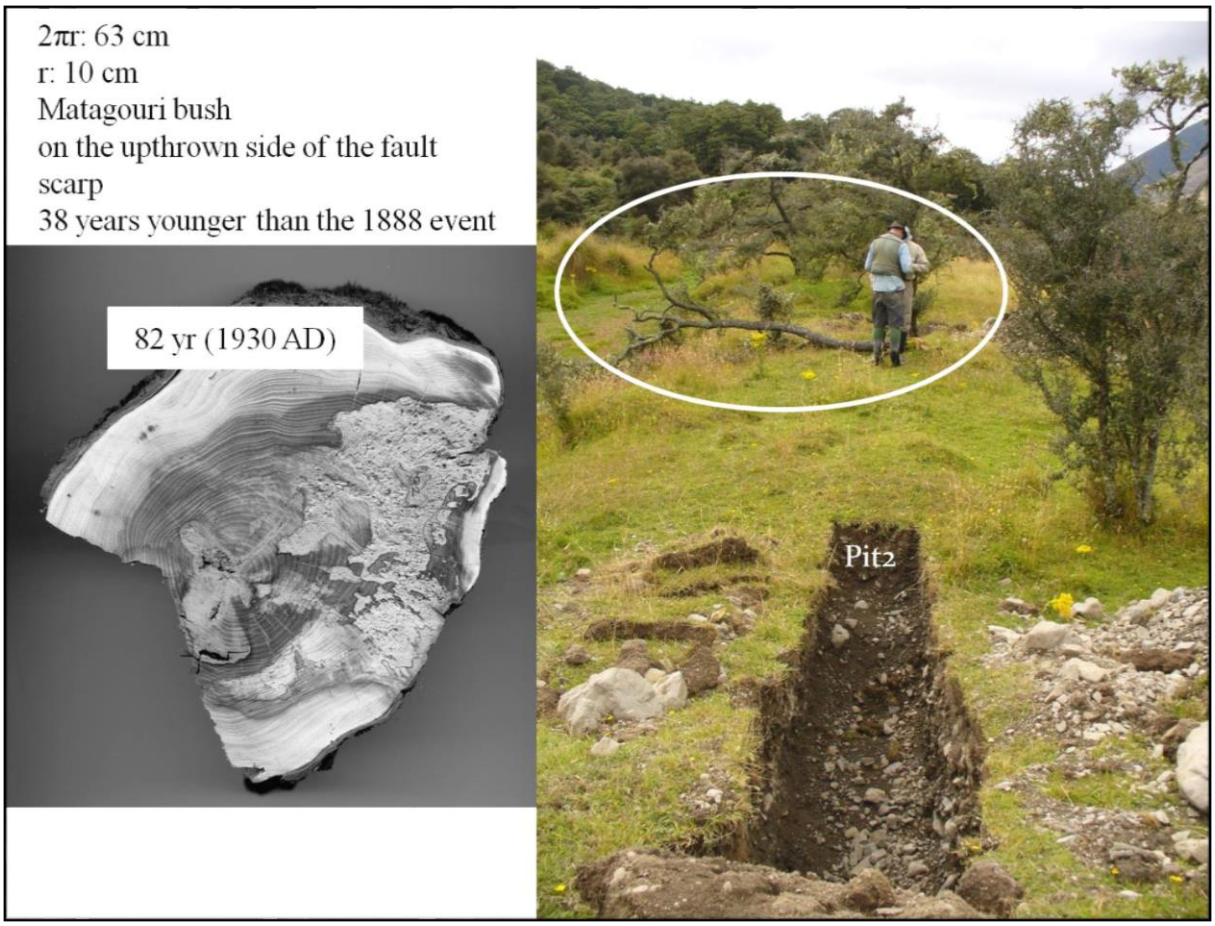

Fig. DR2. The largest Matagouri bush was cut down. The bush has ring count of 82 yr and a colonization age of A.D. ~1930. This probably provides an age related to the clearance of forest at the Hope Shelter it, and gives us no insights into the timing of earthquake there.

Part. 3

Supplementary pit logs

These data are provided as they show extra information about the geomorphology and age of the site. However, the OSL ages from the pits are looking subsequently older than our estimated age of the low gradient fan using the downcutting rate of the Hope River estimated by Cowan (1989) and the height of the fan with respect to the current position of the Hope River.

Pit1 (branch trench)

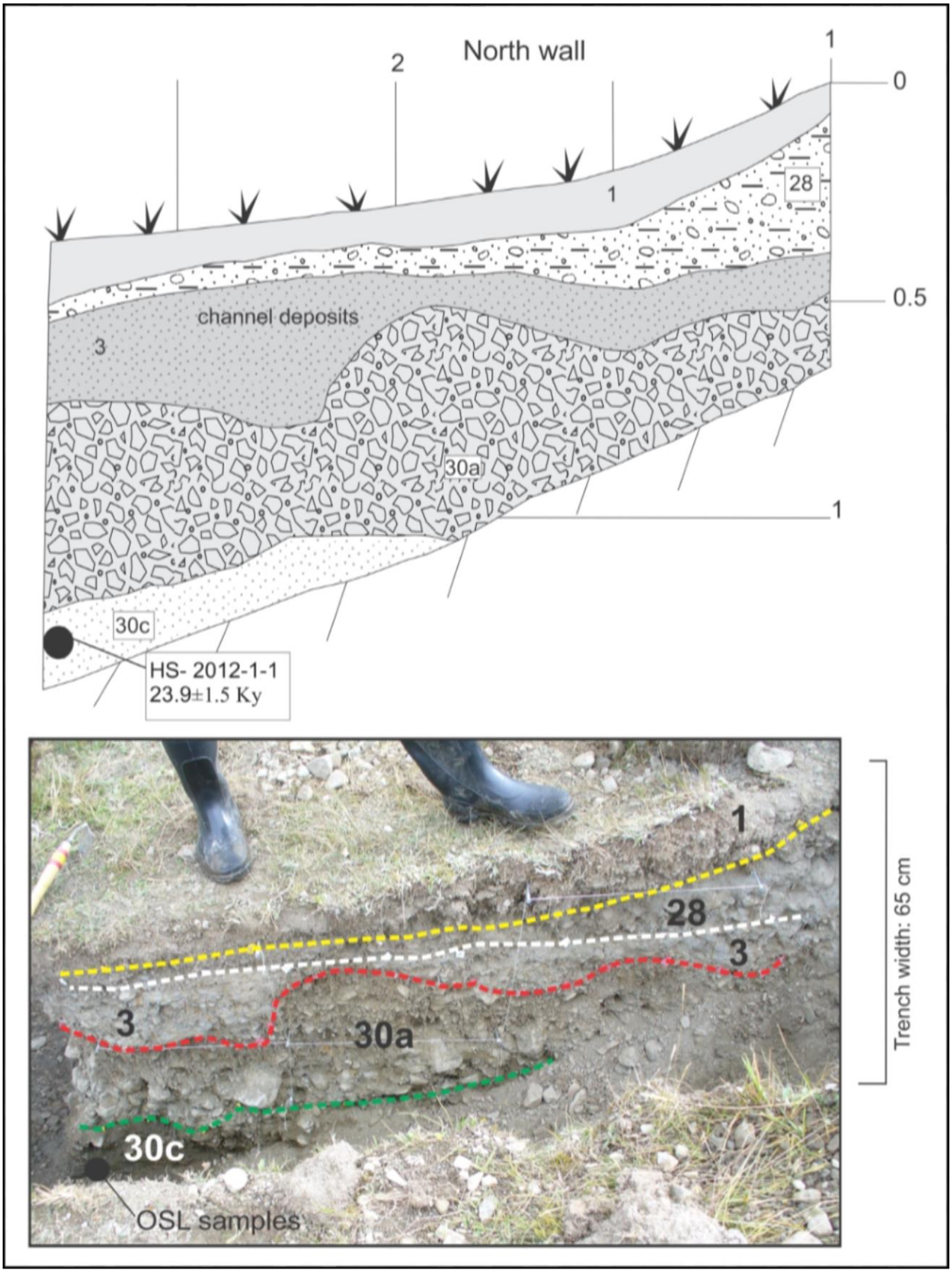

Fig. DR3. Graphic and photo logs of the branch trench (Pit 1). This branch trench was 2.4 m long, 65 cm wide and 0.5-1 m deep. The second unit from top and the lower units are named 28, 30a and 30c respectively because they are correlated with units 28, 30a and 30c in Trench 1. Depositional units are described in section "Unit description of Pit 1". The ground surface marks the cross-sectional profile of the channel forming the wind gap. The current wind gap is erosional, but is underlain by an older channel, filled by unit 3.

Unit 3 shows geometry of the abandoned channel on the fault scarp. One OSL sample was taken from unit 30c at depth 92 cm below the surface to estimate the age of the fan.

Unit description of Pit1:

1-Top soil [soil]

28- Light reddish grey pebbly silty sand, maximum clast size: 7cm, average clast size: 1cm, moderately loose, matrix: loamy sand, some iron oxidation along root traces, gravely loamy (clay, silt, sand) sand [fan alluvium]

3- Sandy silt, subrounded pebbles, some bedding, maximum grain size: 5 cm [channel deposits]

30a- Light olive grey sandy gravel, maximum clast size: 18cm, average clast size: 3cm, matrix: medium-coarse sand, moderately loose, large clast iron stained [fan alluvium]

30c- Dark grey medium to coarse sand, very well sorted, moist [fan alluvium]

Pit3

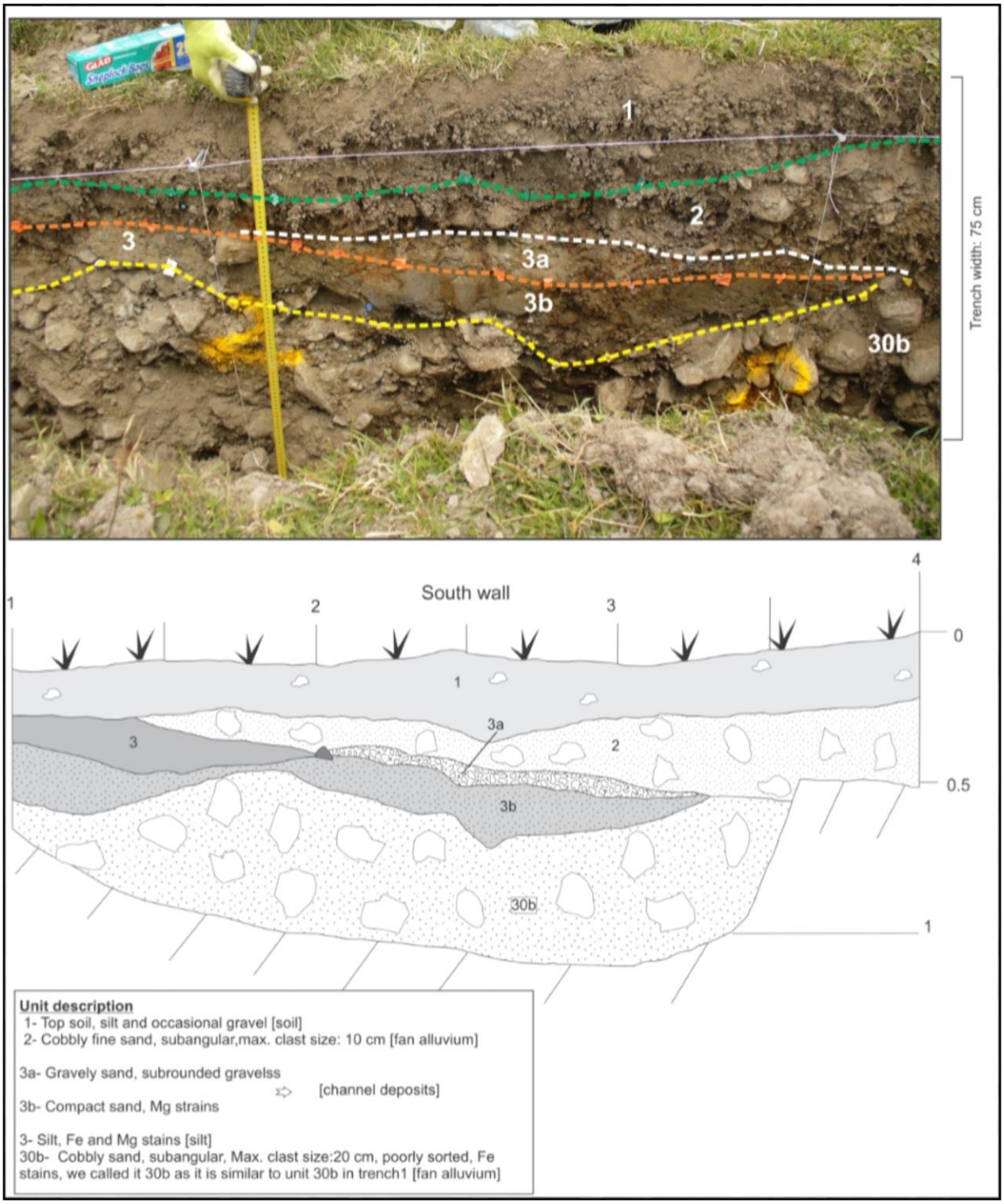

Fig. DR4. Graphic and photo logs of Pit 3. This pit was 3 m long, 75 cm wide and 1 m deep. The lowest unit is named 30b because it is correlated with unit 30b in trench1. Units 3a and 3b show geometry of the abandoned channel on the fault scarp.

Pit4

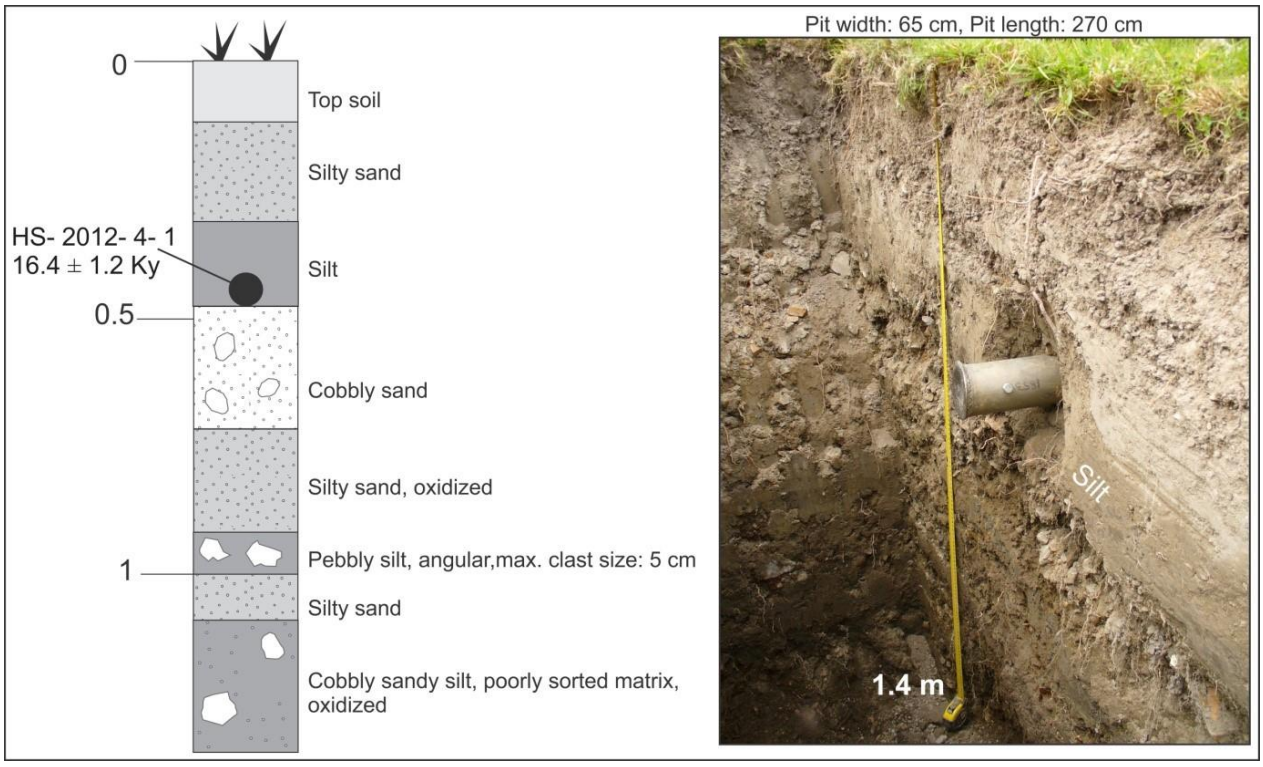

Fig. DR5. Graphic and photo logs of Pit 4. This pit was 2.7 m long, 65 cm wide and 1.4 m deep. Unit description is done on the log. One OSL sample was taken from the silty unit at depth 45 cm below the surface to estimate the age of the fan.

Part. 4

Supplementary information regarding Schmidt Hammering

Schmidt Hammer

The Schmidt hammer (SH) was designed in 1948 to test the hardness of concrete (Goudie, 2006). It has been used in geomorphological studies for relative dating of the Holocene surfaces for nearly four decades (Winkler, 2005; Goudie, 2006, Shakesby et al., 2011). When applied on a rock surface, it measures the rebound (r-value) of a spring-loaded mass impacting against the surface of the rock. The rebound value is dependent to the hardness and compressional strength of the rock surface (Winkler, 2005; Goudie, 2006; Shakesby et al., 2006).

Methodology

In this study, an N-type SH with a calibrated energy of 2.207 Nm was first calibrated and then applied to the surfaces of 75 boulders within a debris deposit near the Hope-Kiwi confluence and 79 boulders within the debris deposit at the Hope Shelter site. Both debris deposits are located ~5 km apart within the Hope Valley and are composed of boulders with the same lithology; i.e., sandstone of the Torlesse formation (Fig. DR6). At each site, one SH impact was implemented on each boulder (Winkler, 2000, 2005, Stahl et al., 2013). We selected very large and stable boulder to prevent boulder movement during tests, and avoided edges of the boulders and surfaces with joints, lichen and moss

(Winkler, 2005). We compared the mean values of the SH from the two deposits using one way ANOVA (analysis of varience). The results are presented in Table. DR1. The results of ANOVA imply no significant age difference between the two groups. However, in relative age dating with SH, a maximum time resolution of ~300 years is common (Winkler, 2005). The mean value of the Hope Shelter deposit is slightly higher (47.4) with respect to the Hope-Kiwi site (46). Taking the slight differences in the mean values of the two sites and the time resolution of the SH into account, it can be concluded that the Hope Shelter debris deposit could possibly be younger (300? yr) than the Hope-Kiwi deposit. However, based on the ANOVA results, we can argue that the two debris deposits could have occurred around the same time in the Hope Valley and they are valuable for earthquake studies.

The appearance of a similar debris deposit near the Hope-Kiwi confluence, which was documented by McKay (1890) following the 1888 event (Figs. 2-3, and Appendix 1: 14), helped us to better understand the debris deposit and forest pattern at the Hope Shelter site. The Hope Shelter debris deposit showed an equivalent Schmidt Hammer mean rebound value to the examined debris deposits (older than the 1888) located near the Hope-Kiwi confluence to the south of the 1888 failure (Fig. DR6). Therefore, our results strongly suggest that the debris deposit at the Hope Shelter site was not generated during the 1888 event, consistent with the dendrochronologic results. Therefore, we allocated a minimum age of ~275 years and a maximum age of <800 years to the Hope Shelter debris deposit based on the minimum age of the trees grown on the debris deposit and the age of the unconformity below unit 12 in T-2 because unit 12 could possibly represent a signal of the debris deposit in the swamp.

The results of this work could be useful for further investigations of paleoearthquakes if combined with accurately dated surfaces nearby the debris deposits and known earthquake chronologies, but by the analysis we have done, we only know that the debris are about the same age.

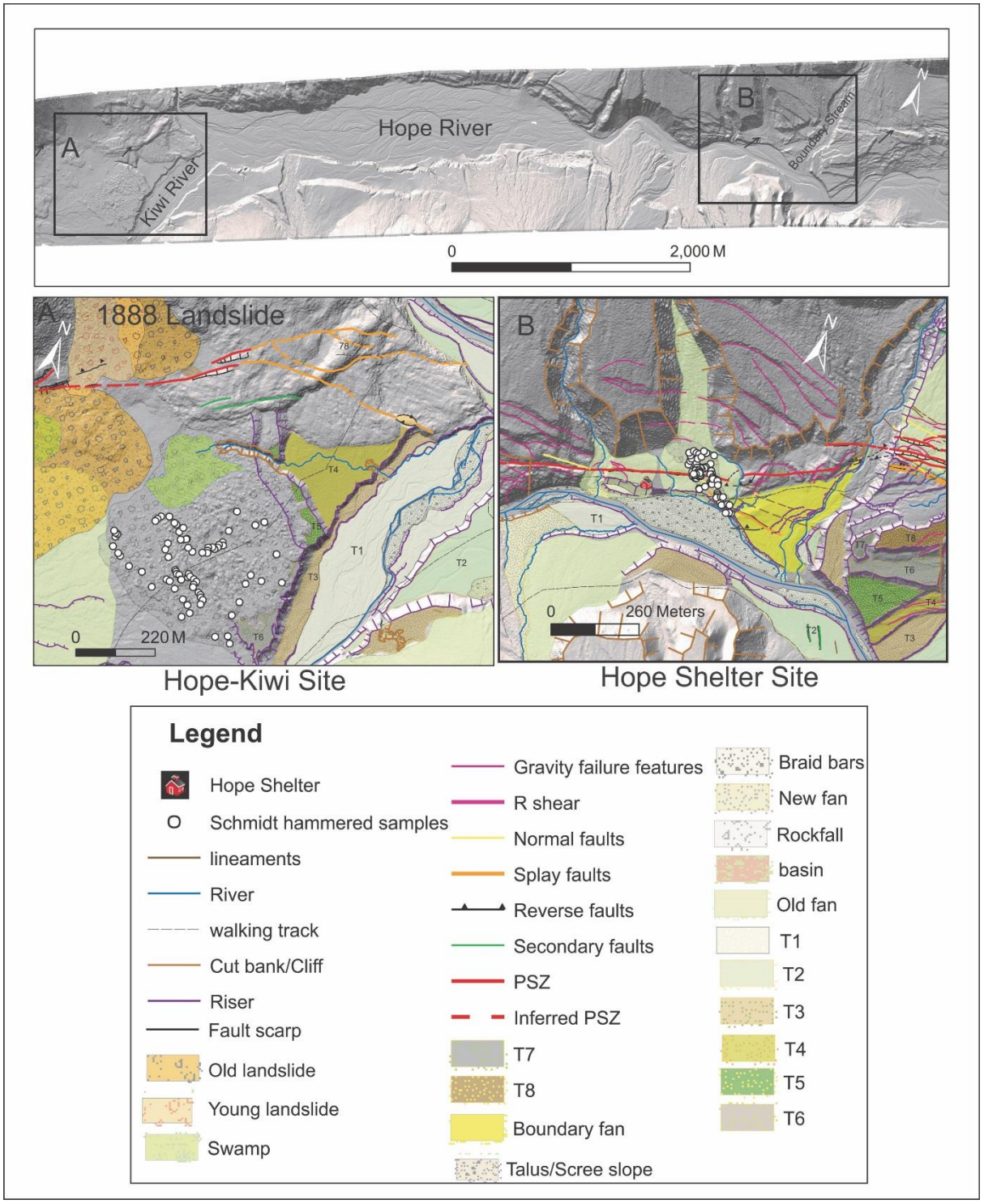

Fig. DR6. Locations of the two sites relative to each other in the Hope Valley are shown on the uninterpreted LiDAR strip. Location of the Schmidt hammered sites are shown on the interpreted windows of LiDAR. Location of the landslide caused by the 1888 earthquake (McKay, 1890) has been shown on A. Black arrows on the uninterpreted LiDAR strip point out to the fault.

Table. DR1. Details of the SH data of the two debris deposits are presented. The results of the ANOVA analysis are also included.

Site	N	R-values: mean	Median	Skewness	Kurtosis	Minimum age of the debris deposit Maximum age of the debris deposits
Hope-Kiwi	75	46	46	0.29	-0.68	N/A
Hope Shelter	79	47.4	48	0.32	0.64	Min ~200 (from dendrochronology) Max ~ 1700 yr (from base of the swamp)

ANOVA results

Descriptive

Groups	N	Mean	Std. Deviation	Std. Error	95% Confidence interval for mean	
					Lower bound	Upper bound
HK	75	46	5.22722	0.60359	44.7973	47.2027
HS	79	47.4051	6.19867	0.69741	46.0166	48.7935
Total	154	46.7208	5.77067	0.46501	45.8021	47.6395

ANOVA

	Sum of squares	df	Mean square	F	Sig.
Between groups	75.956	1	75.956	2.300	0.131
Within groups	5019.038	125			
Total	5094.994	135			

References

Goudie, A. S., 2006, The Schmidt hammer in geomorphological research: Progress in Physical Geography, v. 30, no. 6, p. 703-718.

Shakesby, R. A., Matthews, J. A., Karlén, W., and Los, S. O., 2011, The Schmidt hammer as a Holocene calibrated-age dating technique: Testing the form of the R-value-age relationship and defining the predicted-age errors: Holocene, v. 21, no. 4, p. 615-628.

Shakesby, R. A., Matthews, J. A., and Owen, G., 2006, The Schmidt hammer as a relative-age dating tool and its potential for calibrated-age dating in Holocene glaciated environments: Quaternary Science Reviews, v. 25, no. 21-22, p. 2846-2867.

Stahl, T., Winkler, S., Quigley, M., Bebbington, M., Duffy, B., and Duke, D., 2013, Schmidt hammer exposure-age dating (SHD) of late Quaternary fluvial terraces in New Zealand: Earth Surface Processes and Landforms, v. 38, no. 15, p. 1838-1850.

Winkler, S., 2005, The Schmidt hammer as a relative-age dating technique: Potential and limitations of its application on Holocene moraines in Mt Cook National Park, Southern Alps, New Zealand: New Zeal J Geol Geop, v. 48, no. 1, p. 105-116.

Part. 5

Supplementary information regarding the fault bend

Fig. DR7. A huge displaced boulder was found at the base of the fault scarp near the fault bend. Location: ~2.8 km from Boundary stream towards east at ~ X and Y: 1545892.667 and 5282807.323 (Reference: NZGD_2000_TM) respectively.

Fig. DR8. Fallen boulders were found at the base of the fault scarp (within the basin) near the fault bend. Location: ~2.7 km from Boundary stream towards east at approximate X and Y: 154511.79 and 5282879.733 (Reference: NZGD_2000_TM) respectively. Scarp height is ~5 m. Basin width is 22.2 m. Picture was taken in January 2012.

Part. 6

Supplementary information regarding Parakeet Stream site

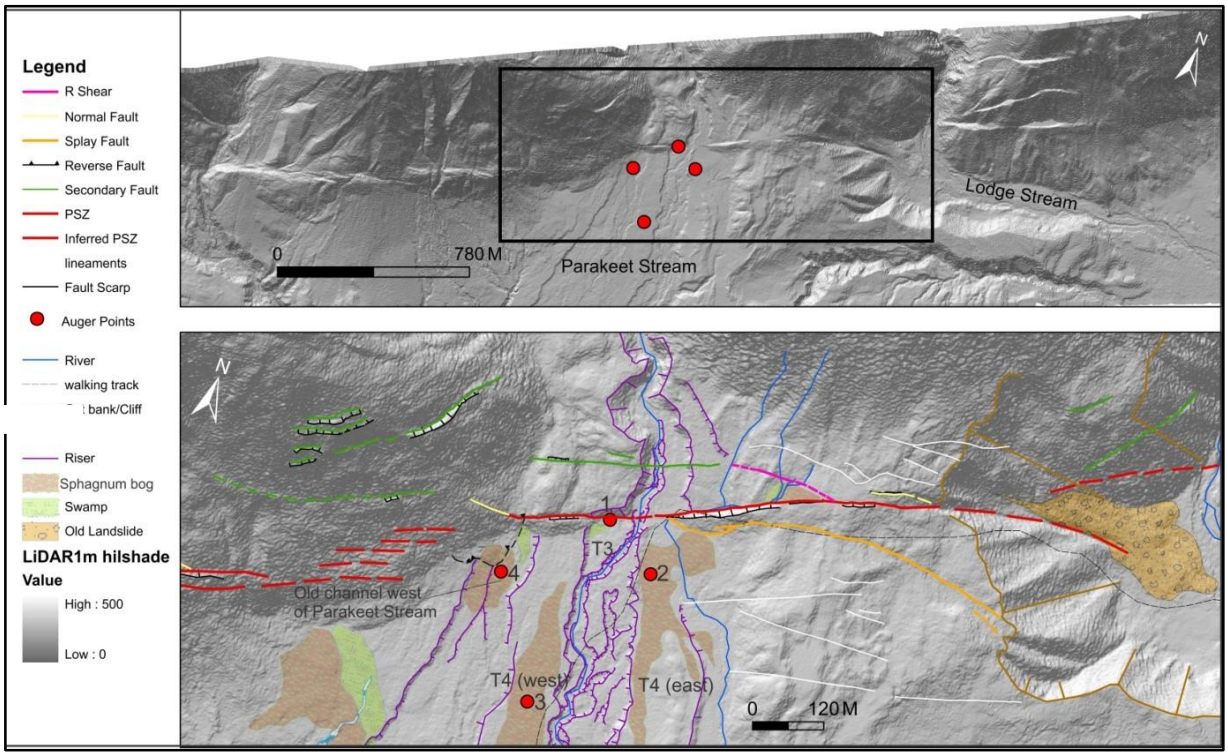

Fig. DR9. Uninterpreted and interpreted LiDAR hillshade model of the Parakeet Stream site. Location: ~4 km west of the Hope-Kiwi confluence. Closed Red circles show the augur points (pits). Abbreviation PSZ: Principal Slip Zone. Term "old landslide" was used in the legend because the landslide deposit was colonised by very old beech trees. Secondary Faults are parallel to subparallel faults to the PSZ with dextral and or vertical displacements. Lineaments are the faults with no discernible displacement. All the pits and auger holes were excavated into the sphagnum bog surfaces.

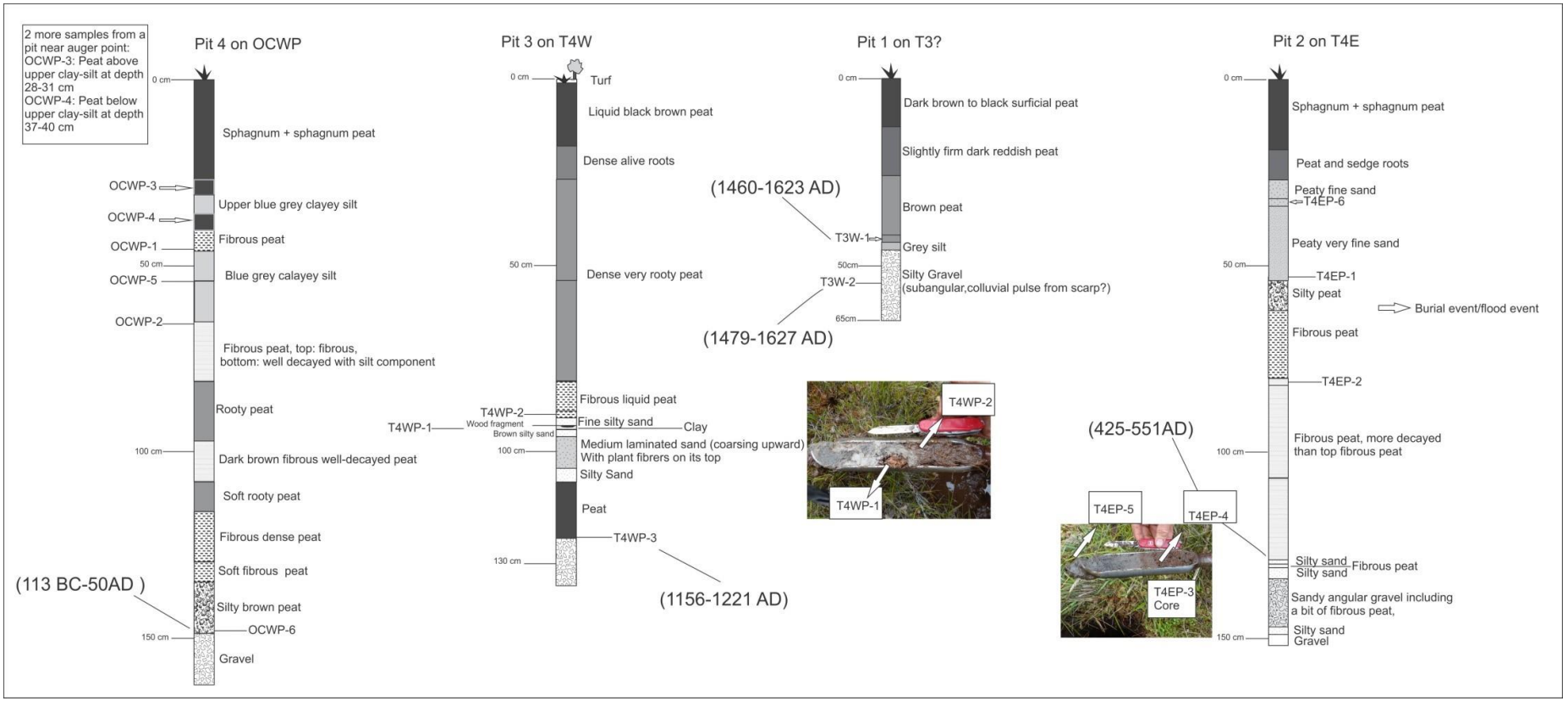

Fig. DR10. Pit logs at the Parakeet Stream site. We collected samples from every peat horizon as indicated. In total, five samples were C-14 dated from the logs. These samples are from the deepest parts of the pits, above the gravel units, to identify the maximum ages of the swamps. The dated samples display the minimum age for the gravel deposit.

Fallen boulder due to the coseismic shaking associated with the 1888 event?

At the base of the fault scarp, on the surface of terrace T3 (Fig. DR9), we found a large spheroid boulder (Fig. DR11). The boulder was situated on a fallen tree. We found a young Silver beech grown on the fallen tree. The young tree was cut down at 46 cm height from its base. The tree postdates the 1888 event. As it normally takes 17-47 years for beech trees to colonize at high elevation or slopping surfaces (Langridge et al. 2007), this probably provides evidence for severe shaking at the Parakeet Stream site during the 1888 event; however, it does not give us any direct insight into the 1888 surface rupture extension.

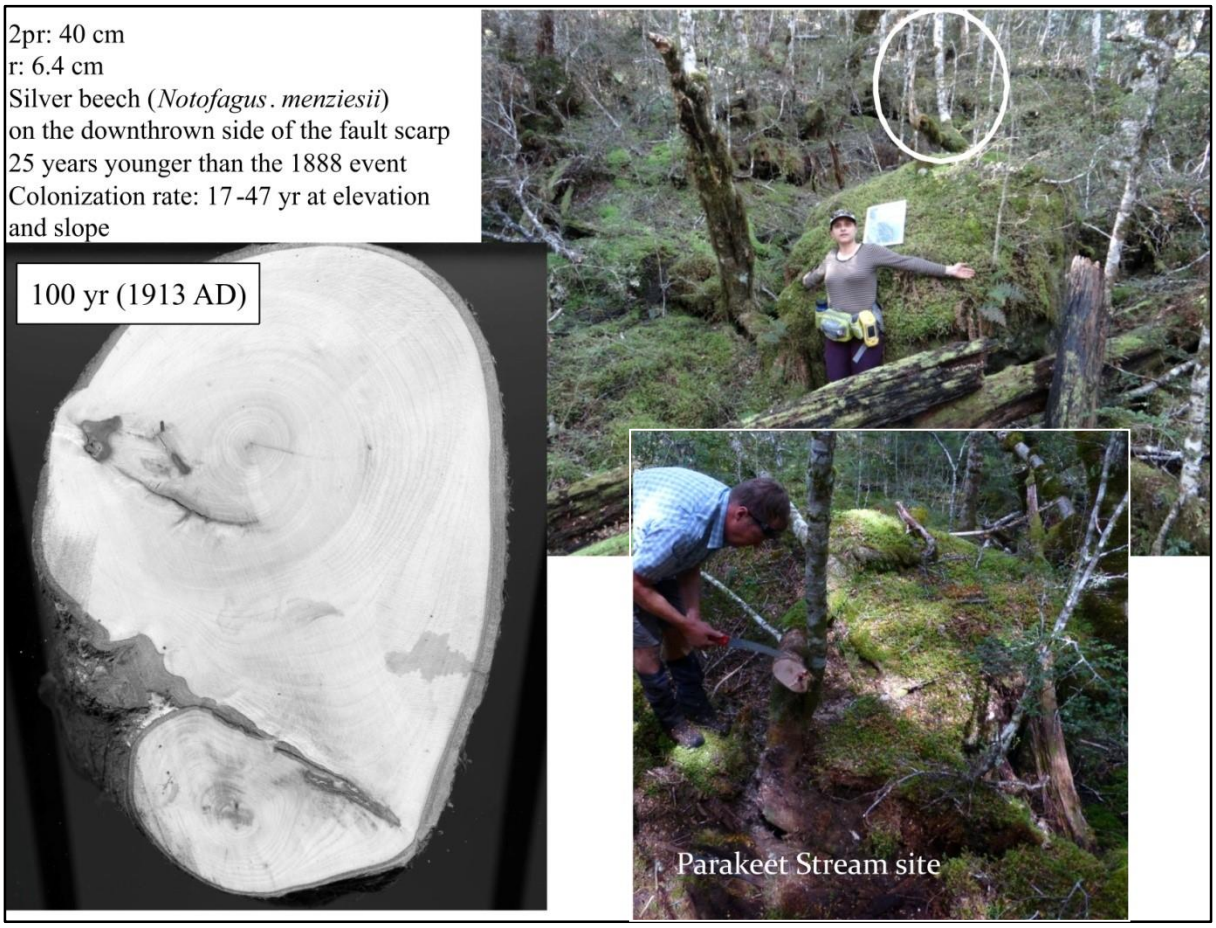

Fig. DR11. The young Silver beech was cut down. The tree has ring count of 100 yr and a colonization age of A.D. ~1913.

References

Langridge, R., Duncan, R., and Almond, P., 2007, Indicators of recent paleoseismic activity along the western Hope Fault: GNS Science Consultancy Report 2006/151, p. 99.+appendices.

Part. 7

Supplementary information regarding calculating the mean recurrence interval and its uncertainty for our preferred earthquakes timings

To estimate the mean recurrence interval (MRI) and its uncertainty, we followed the methodology employed by Parsons (2008), and the calculations used by Nicol et al. (2012). In calculate the MRI, the Monte Carlo procedure is used to generate a recurrence interval histogram from earthquake input data. In this study, event timings of the earthquakes and their uncertainties, presented in years before 2013 (i.e., sampling year), were used in the calculations. The recurrence interval histogram for the Hurunui segment of the Hope fault is shown in Fig. DR12. The MRI (~298 years) and Standard deviation (~199 years) calculated from the histogram are presented in Table. DR2. The uncertainty in the MRI is the Standard deviation divided by the square root of the number of intervals. Based on this analysis, the MRI is reported 298 ± 88 years. The associated uncertainty includes both process and dating uncertainties.

Events timing	**Event timing (presented in years before 2013) with uncertainty**
1-E1 (1888)	1- 125±1
2-E2 (1740-1840)	2- 223±50
3-E3 (1479-1609)	3- 462±72
4-E4 (819-1092)	4- 1057±137
5-E5 (439-551)	5- 1518±56
6-E6 (373-419)	6- 1617±23

Differences

1- E1-E2= 98

2- E2-E3=239

3- E3-E4= 595

4- E4-E5=461

5- E5-E6=99

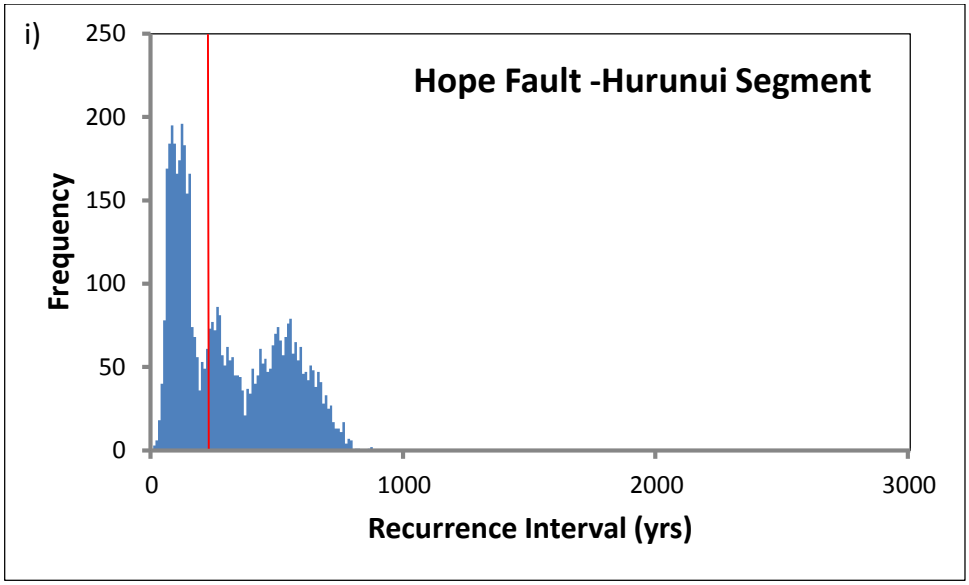

Fig. DR12. Recurrence interval histogram for the Hurunui segment of the Hope fault generated using the earthquake data and the Monte Carlo method.

Table. DR2. Calculated parameters from the histogram generated by the Monte Carlo procedure. The MRI and Standard deviation are highlighted.

Mean	generated mean	generated mode	generated median	generated min	generated max	generated stdev	Min	Max	Stdev	Events
298.4	298.1550849		247.00	3.53130725	863.6074743	207.3594521	98	588	**198.9267**	6

References

Parsons, T., 2008, Monte Carlo method for determining earthquake recurrence parameters from short paleoseismic cataloges: Example calculations from California: Journal of geophysical research, v. 113, no. B03302

Nicol, A., Robinson, R., Van Dissen, R. J., and Harvison, A., 2012, Variability of single event slip and recurrence intervals for large magnitude paleoearthquakes on New Zealand's active faults: GNS Science Report 2012/41, p. 57 p.